

Semiconductor phonon and charge transport Monte Carlo simulation using Geant4

D. Brandt¹, R. Agnese², P. Redl³, K. Schneck¹, M. Asai¹, M. Kelsey¹, D. Faiez⁴, E. Bagli⁵, B. Cabrera³, R. Partridge¹, T. Saab², B. Sadoulet⁴,

Abstract

A phonon and charge transport simulation based on the Geant4 Monte Carlo toolkit is presented. The transport code is capable of propagating acoustic phonons, electrons and holes in cryogenic crystals. Anisotropic phonon propagation, oblique carrier propagation and phonon emission by accelerated carriers are all taken into account. The simulation successfully reproduces theoretical predictions and experimental observations such as phonon caustics, heat pulse propagation times and mean carrier drift velocities.

Implementation of the transport code using the Geant4 toolkit ensures availability to the wider scientific community.

Keywords: Geant4, Phonon, Electron/Hole transport, Cryogenic detectors

1. Introduction

We present a Monte Carlo simulation of phonon and charge transport in semiconductor crystals using Geant4. Geant4 is a sophisticated C++ based Monte Carlo simulation toolkit maintained by an international collaboration and freely available under an open source license [2, 3]. The toolkit was originally developed in support of High Energy Physics (HEP) experiments and provides a framework for simulating the passage of particles through complex geometries and materials. It aims to accurately simulate all particle-matter interactions and has become an important tool both for HEP particle accelerator based experiments, and experiments wishing to estimate backgrounds induced by cosmic rays and from radiogenic sources [4, 5].

In its current incarnation, the Geant4 toolkit is entirely focused on free particles and does not take into account crystal physics or conduction/valence band interactions of the low-energy charge carriers and phonons relevant to condensed-matter physics. This paper documents our effort to build a cohesive Geant4 Condensed Matter Physics Monte Carlo simulation toolkit,

G4CMP. The original purpose of this project was to accurately reproduce data from the Cryogenic Dark Matter Search (CDMS) [7, 8, 9], a dark-matter direct-detection experiment. The CDMS detectors are cylindrical Ge crystals approximately 75 mm in diameter with a height of 25 mm [10], cooled to approximately 60 mK. Dark-matter particles may recoil from Ge nuclei and thus create phonons and electron-hole pairs within the crystal [6]. Electron-hole pairs drift in a few V/cm field to the crystal faces where they are collected. Phonons are detected by superconducting Transition Edge Sensors (TES) [1]. We reproduce all of these processes in our simulation. The phonon and charge transport code described below models several physics processes relevant to phonon and charge collection at cryogenic temperatures. This includes anisotropic phonon transport and focusing, phonon isotope scattering, anharmonic downconversion, oblique charge carrier propagation with inter-valley scattering, and emission of Luke-Neganov phonons by accelerated carriers. The resulting G4CMP framework is sufficiently general that it should be useful to other experiments employing cryogenic phonon and/or ionization detectors.

2. Phonon Transport

Phonon transport was the first component of the G4CMP framework to be developed [5]. Since the phonon transport code described here is intended for

¹SLAC National Accelerator Laboratory, Menlo Park, CA, USA

²University of Florida, Gainesville, FL, USA

³Stanford University, Stanford, CA, USA

⁴University of California Berkeley, Berkeley, CA, USA

⁵University of Ferrara, Ferrara, Italy

⁶Massachusetts Institute of Technology, Cambridge, MA, USA

temperatures $T < 1K$, scattering off thermally excited background phonons is ignored. Currently, only acoustic phonons are simulated, with optical phonons not supported.

2.1. Anisotropic transport and phonon focusing

Phonons are quantized vibrations of the crystal lattice. The propagation of phonons is governed by the three-dimensional wave equation [13]:

$$\rho\omega^2 e_i = C_{ijml} k_j k_m e_l, \quad (1)$$

where ρ is the crystal mass density, ω is the angular phonon frequency, \vec{e} is the polarization vector, \vec{k} is a wave vector and C_{ijml} is the elasticity tensor.

For any given wave vector, \vec{k} , Eq. 1 has three eigenvalues, ω , and three eigenvectors, \vec{e} . These correspond to the three different polarization states: Longitudinal (L), Fast Transverse (FT) and Slow Transverse (ST). The actual direction and velocity of propagation of phonons is given by the group velocity vector $\vec{v}_g = d\omega/dk$. The group velocity can be calculated by interpreting ω in Eq. 1 as a function of \vec{k} :

$$\vec{v}_g = \nabla\omega(\vec{k}), \quad (2)$$

Due to the anisotropy in C_{ijml} , Eq. 2 yields a group velocity \vec{v}_g that is not parallel to the phonon momentum $\hbar\vec{k}$. Instead, phonons are focused onto propagation directions that correspond to the highest density of eigenvectors \vec{k} . This focusing gives rise to caustics when observing the energy distribution resulting from a point-like phonon source that is isotropic in \vec{k} -space. The resulting caustics can be observed using microcalorimeters [12]. Figure 1 shows that the caustics simulated by the Geant4 phonon transport code are in good agreement with experimental observations.

For the purposes of the G4CMP phonon transport code, the wave equation is not solved in real time. Instead, a look-up table is generated which maps \vec{k} onto \vec{v}_g , and bilinear interpolation is used to generate a continuous mapping function. Phonon focusing and methods for solving the three-dimensional wave equations are treated in [13].

2.2. Phonon processes

In addition to the phonon equation of motion, Eq. 1, two processes are relevant to acoustic phonon transport in cryogenic crystals: isotope scattering and anharmonic downconversion [14, 15, 16]. The scattering and

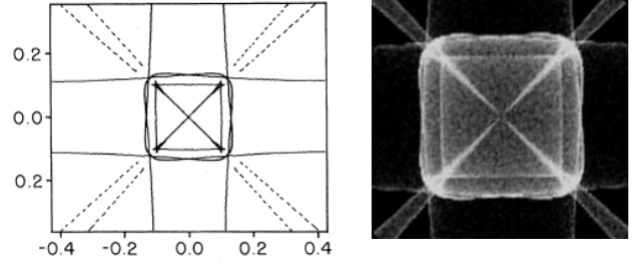


Figure 1: **Left:** outline of phonon caustics in Ge as predicted by Nothrop and Wolfe [12]. **Right:** Phonon caustics as simulated using the Geant4 phonon transport code. This result is in good agreement with both the theoretical prediction and experimental observations reported by Nothrop and Wolfe [12].

downconversion rates for phonons in a cryogenic crystal are given by [5, 15]:

$$\Gamma_{\text{anh}} = A\nu^5, \quad (3)$$

$$\Gamma_{\text{scatter}} = B\nu^4, \quad (4)$$

where Γ_{anh} is the number of anharmonic downconversion events per unit time, Γ_{scatter} is the number of scattering events per unit time, ν is the phonon frequency and A , B are constants of proportionality related to the elasticity tensor. In Ge, $A = 6.43 \times 10^{-55} \text{ s}^4$ and $B = 3.67 \times 10^{-41} \text{ s}^3$ [5, 14].

Isotope scattering occurs when a phonon interacts with an isotopic substitution site in the lattice. It is effectively an elastic scattering during which the phonon momentum vector is randomized, and the phonon polarization state can change freely between the three states L , ST , FT . The partition between the three polarizations is determined by the relative density of allowed states for each polarization. This change between polarization states is often referred to as *mode mixing*.

Anharmonic downconversion causes a single phonon to decay into two phonons of reduced energy. This process conserves energy but not momentum, since momentum is exchanged with the crystal lattice. In theory all three polarization states can decay; however, the downconversion rate of L -phonons completely dominates the energy evolution of the phonon system, with downconversion events from other polarization states being negligible [15].

Equations 3 and 4 indicate that both process rates strongly depend on phonon energy $\hbar\nu$. High-energy phonons (ν of order THz) start out in a diffusive regime with high isotope scattering and downconversion rates and mean free paths of order microns. Once a few downconversion events have occurred, phonon mean free paths increase to be of order $\sim 0.1 \text{ m}$ (the size of

a typical CDMS detector). This transition from a diffuse to a ballistic transport mode is commonly referred to as “quasi-diffuse” and controls the time evolution of phonon pulses. Simulation of phonon pulses with our Geant4 transport code as described in [5] shows good agreement with experiment. Anharmonic downconversion and isotope scattering are well understood and are discussed in great detail in the literature [14, 15, 13, 16].

3. Charge Transport

In addition to the phonon physics described above, the G4CMP framework enables simulation of charge propagation through germanium crystals, for which there are three processes to consider: acceleration by an applied electromagnetic field, inter-valley scattering, and emission of Neganov-Luke phonons.

3.1. Neganov-Luke Phonons

As the charge carriers are accelerated through the crystal, they emit phonons in a process that is analogous to Cerenkov radiation. Because electrons and holes have different effective mass properties in germanium, Neganov-Luke phonon emission is implemented differently for each type of charge carrier, as explained below.

3.1.1. Holes

The effective mass of a hole in germanium is a scalar, so its propagation is simply that of a charged particle in vacuum with an applied field.

Hole-phonon scattering is an elastic process, conserving energy and momentum, as shown in Fig. 2. From

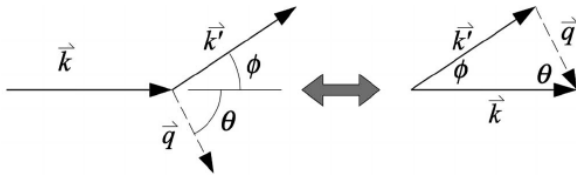


Figure 2: A charge carrier has initial wavevector \vec{k} and emits a Neganov-Luke phonon with wavevector \vec{q} [17]

conservation of energy and momentum,

$$k'^2 = k^2 + q^2 - 2kq \cos \theta, \quad q = 2(k \cos \theta - k_L), \quad (5)$$

with k_L defined as $k_L = mv_L/\hbar$, where v_L is the longitudinal phonon phase speed and m is the effective mass of the hole [18]. Solving for ϕ ,

$$\cos \phi = \frac{k^2 - 2k_L(k \cos \theta - k_L) - 2(k \cos \theta - k_L)^2}{k \sqrt{k^2 - 4k_L(k \cos \theta - k_L)}}, \quad (6)$$

where $k_L = mv_L/\hbar$. Using Fermi's Golden Rule, we can determine a scattering rate [17]

$$1/\tau = \frac{v_L k}{3l_0 k_L} \left(1 - \frac{k_L}{k}\right)^3, \quad (7)$$

with an angular distribution,

$$P(k, \theta) d\theta = \frac{v_L}{l_0} \left(\frac{k}{k_L}\right)^2 \left(\cos \theta - \frac{k_L}{k}\right)^2 \sin \theta d\theta, \quad (8)$$

where $0 \leq \theta \leq \arccos k_L/k < \pi/2$ and l_0 is a characteristic scattering length defined as $l_0 = \frac{\pi \hbar^4 \rho}{2m^3 C^2}$ with C being the deformation potential constant for Ge [17].

3.1.2. Electrons

Unlike the hole, the electron has a tensor effective mass in germanium. Some transformations need to be applied before propagating the electron through the crystal.

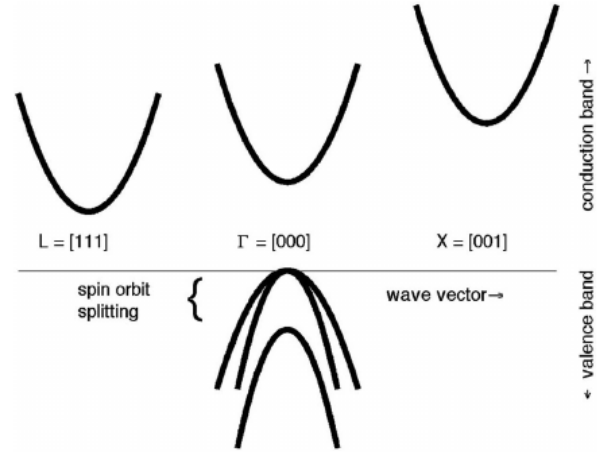


Figure 3: Conduction and valence bands in Ge. At present, the G4CMP framework only simulates electrons propagating in the direction of the L conduction band. At sufficiently low temperature and applied field, this approximation is accurate [17].

For a coordinate system with one axis aligned with the principal axis of the conduction valley, the electron's equation of motion is

$$\frac{eE_i}{m_i} = \frac{dv_i}{dt}. \quad (9)$$

However, so that we can apply the same Neganov-Luke phonon emission recipe to electrons as holes, we need to transform to a coordinate system in which the constant energy surfaces are spherical. In that space, $v_i^* =$

$v_i/\sqrt{m_c/m_i}$, where m_c is given by $3/m_c = 1/m_{\parallel} + 2/m_{\perp}$. And so,

$$\frac{eE_i^*}{m_c} = \frac{dv_i^*}{dt}, \quad (10)$$

Once the coordinate system is rotated into the conduction valley frame, a Herring-Vogt transformation is applied,

$$T_{HV} = \begin{pmatrix} \sqrt{\frac{m_c}{m_{\parallel}}} & 0 & 0 \\ 0 & \sqrt{\frac{m_c}{m_{\perp}}} & 0 \\ 0 & 0 & \sqrt{\frac{m_c}{m_{\perp}}} \end{pmatrix}, \quad (11)$$

From this space, the same recipe that applied to holes for Neganov-Luke phonon emission can be followed for electrons [17].

3.2. Inter-Valley Scattering

Electron propagation, as discussed in the previous section, has one particularly interesting feature that electrons propagate through the crystal in one of four distinct valleys [17, 18]. Electrons are not bound to those valleys permanently, however, and can scatter between valleys. This process is known as inter-valley scattering and occurs in one of two ways: an electron scatters off the lattice or off an impurity [19]. The rate for both processes is dependent on the electric field strength, with lattice scattering being the dominant factor in larger fields ($\gtrsim 5$ V/m), while impurity scattering dominates in lower fields (~ 1 V/m). The EDELWEISS [20] collaboration determined the scattering rates as a function of the electric field for typical Ge crystals [19]. We used the results obtained in these studies to set the inter-valley scattering amplitude in the Geant4 framework and compare it to previous implementations of the charge transport code [17, 18]. The result of electrons and holes propagating through 2.54 cm of Ge in an 0.5 V/m electric field is shown in Fig. 4. The top two panels show the result with inter-valley scattering turned on while the bottom two panels show the result for inter-valley scattering turned off. The panels on the right show the results for the legacy (MATLAB-based) simulation [17, 18] with somewhat fewer statistics than the Geant4 simulations. The bottom two panels also show hole transport through the crystal for the Geant4 and legacy simulations [17, 18].

3.3. Charge Carrier Drift Speed Results

As the charge carriers are accelerated by the electric field, they emit Neganov-Luke phonons. For different values of the applied electric field, a maximum

drift speed of the carrier is reached, where the energy gained from the electric field is canceled by the energy lost from emission of phonons. Fig. 5 shows the average drift velocities of electrons and holes in the G4CMP package with experimental data [21] and the theoretical curve [22] on which the Monte Carlo is based.

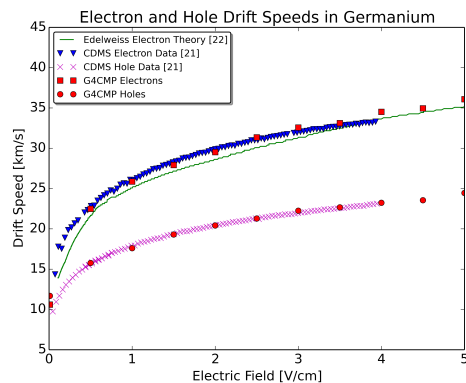


Figure 5: Comparison of the G4CMP charge code with various data and models.

4. Conclusion

We have presented a new Monte Carlo transport code capable of propagating phonons on a cryogenic crystal lattice (Section 2) as well as drifting electron-hole pairs, taking into account conduction band anisotropy (Section 3). The results produced by the transport code are in good agreement with experiment, reproducing phonon caustics and carrier drift velocity with acceptable accuracy. It was shown that this code reproduces heat-pulse propagation and dispersion in cryogenic Ge crystals with acceptable accuracy in [5]. The entire transport code is written in C++ for Geant4 and is easily adaptable for crystals other than Ge, provided that the Herring-Vogt contracted elasticity tensor and effective carrier masses are known. The Geant4 framework makes it possible to extend the code presented here. The phonon transport code is already freely available as part of the examples provided with Geant4 v9.6p02 and newer. We hope that the work presented here will establish Geant4 as a tool in condensed-matter physics and cryogenic calorimeter design as well as motivate others to add to the G4CMP framework.

We would like to thank members of the CDMS Detector Monte Carlo Group for discussions that have made completing this work possible. Specifically we want to thank P.L. Brink, A. Anderson and C. Schlupf.

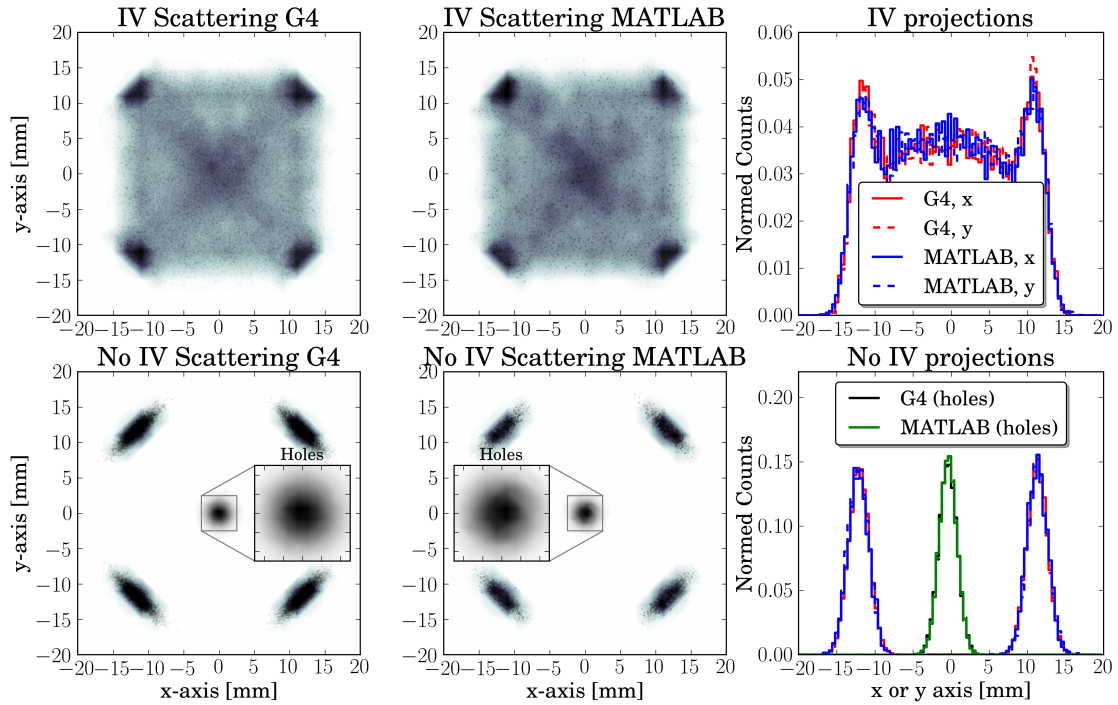


Figure 4: **Left:** Geant4 simulations **Right:** legacy MATLAB simulations. **Top Row:** Simulations with inter-valley scattering turned on, **Bottom Row:** Simulations with inter-valley scattering turned off, including hole transport through the crystal.

Furthermore we would like to thank A. Phipps and K. Sundqvist for useful discussions and providing us with experimental data. S. Yellin and R. Bunkers' on point feedback on earlier paper drafts have helped us improve the final paper tremendously. This work is supported in part by the National Science Foundation and by the United States Department of Energy. SLAC is operated under Contract No. DE-AC02-76SF00515 with the United States Department of Energy.

References

- [1] K. D. Irwin, S. W. Nam, B. Cabrera, B. Chugg and B. Young, *Rev. Sci. Instrum.* **66**, 5322, (1995).
- [2] J. Allison et al., *IEEE Transactions on Nuclear Science* **53**, 270 - 278, (2006).
- [3] S. Agostinelli et al., *Nuclear Instruments and Methods A* **506**, 250 - 303, (2003).
- [4] D.S. Akerib et al., *Phys. Rev. D* **72**, (2005).
- [5] D. Brandt et al., *Journal of Low Temperature Physics* **167**, 485 - 490, (2011).
- [6] Smith, P.F. and Lewin, J.D., *Phys.Rept.* **187**, 203, (1990).
- [7] Z. Ahmed et al., *Science* **327**, 1619, (2010).
- [8] Z. Ahmed et al., *Phys. Rev. D* **84**, 011102, (2011).
- [9] C. Collaboration et al., *arXiv astro-ph* **1304.4279**, (2013).
- [10] R. Agnese et al., *arXiv astro-ph* **1305.2405**, (2013).
- [11] P. Brink et al., *NIM A* **2**, 414, (2006).
- [12] G.A. Nothrop and J.P. Wolfe, *Phys. Rev. Lett.* **19**, 1424, (1979).
- [13] J.P. Wolfe, *Imaging Phonons, Chapter 2,42*, Cambridge University Press, United Kingdom (1998).
- [14] S. Tamura, *Journal of Low Temperature Physics* **93**, 433, (1993).
- [15] S. Tamura, *Phys. Rev. B.* **48**, 13502, (1993).
- [16] S. Tamura, *Phys. Rev. B.* **31**, (1985).
- [17] S. W. Leman, *Rev. Sci. Instrum.* **83**, 091101, (2012).
- [18] Cabrera, B. et al., *arXiv astro-ph* **1004.1233**, (2010).
- [19] Broniatowski, A., *Journal of Low Temperature Physics*, **167**, (2012).
- [20] Juillard, A., *Journal of Low Temperature Physics*, **151**, (2008).
- [21] A. Phipps, K. M. Sundqvist, A. Lam, B. Sadoulet, *Journal of Low Temperature Physics*, **167**, (2012).
- [22] V. Aubry-Fortuna, *AIP Conference Series*, **1185** 639, (2009).